energies

MDPI

Article

An Assessment of the Performance and Emissions of an Otto Power Generator Group Operating with Wet Ethanol at a High Volumetric Compression Ratio

Vinícius Guerra Moreira, Sérgio de Morais Hanriot *, Tales Nazareno, Bruno Eustáquio Pires Ferreira, Rafael Motter Juliatti, Hairton Júnior José da Silveira and Cristiana Brasil Maia

Department of Mechanical Engineering, Pontifical Catholica University of Minas Gerais, Belo Horizonte 30535-901, Brazil; viniciusguerra@pucminas.br (V.G.M.); talesnazareno@gmail.com (T.N.); rafaelmotter@gmail.com (R.M.J.); hairtonjjsilveira@gmail.com (H.J.J.d.S.); cristiana@pucminas.br (C.B.M.)
* Correspondence: hanriot@pucminas.br

Abstract: This work presents an experimental study of the performance and emissions of an internal combustion engine operating in the Otto cycle with a high volumetric compression ratio (17:1). The engine was initially fueled with the standard ethanol used in Brazil, with 7% distilled water (E93W07); we then studied the effects of using different ethanol-in-water mixtures, or 'wet ethanol', with 17%, 27%, 37%, and 47% distilled water concentrations. The tests were carried out with power loads of 5.0–25.0 kW at 5.0 kW intervals and with power loads of 27.5–35.0 kW at 2.5 kW intervals, whether by adding up the loads or by taking them away. The ignition timing was changed to evaluate each load imposed on the engine to avoid knocking. Specific fuel consumption (SFC), brake thermal efficiency (BTE), carbon dioxide emissions (CO_2), carbon monoxide (CO), nitrogen oxides (NO_x), and total hydrocarbon content (THC), as well as the internal pressure in the cylinder and the heat release rate, were measured, and the results are compared. The results show a reduction in CO and NO_x and an increase in THC emissions. However, there were no significant changes in CO_2 emissions when the distilled water percentage in ethanol increased. Regarding the brake thermal efficiency, it was observed that it remained approximately constant for all blends, with the same load being applied to the engine shaft, reaching a maximum value of 35%. The results obtained confirm the technical feasibility of operating an internal combustion engine in the Otto cycle with a high volumetric compression ratio using ethanol with up to 47% distilled water without significant loss of performance.

Keywords: power generation group; biofuel; wet ethanol; performance; emissions; high compression

check for updates

Citation: Moreira, V.G.; Hanriot, S.d.M.; Nazareno, T.; Ferreira, B.E.P.; Juliatti, R.M.; Silveira, H.J.J.d.; Maia, C.B. An Assessment of the Performance and Emissions of an Otto Power Generator Group Operating with Wet Ethanol at a High Volumetric Compression Ratio. *Energies* **2024**, *17*, 6187. https://doi.org/10.3390/en17236187

Academic Editor: Giovanni Lutzemberger

Received: 10 November 2024
Revised: 30 November 2024
Accepted: 5 December 2024
Published: 8 December 2024

Copyright: © 2024 by the authors. Licensee MDPI, Basel, Switzerland. This article is an open access article distributed under the terms and conditions of the Creative Commons Attribution (CC BY) license (https://creativecommons.org/licenses/by/4.0/).

1. Introduction

The search for more sustainable alternative energy solutions is a global necessity. International agreements, such as the Paris Agreement, outline carbon emission reduction targets to mitigate the effects of climate change [1]. To address the increasing demand from the aviation and transport sectors, the implementation of alternative fuels is essential for reducing pollution and promoting environmental sustainability [2]. The use of biofuels in combustion at low temperatures shows great potential to reduce the emissions of CO, THC, and NO_x [3]. Due to its characteristics of retaining oxygen and having a high octane number, anhydrous ethanol can be considered to be one of the main alternatives to fossil fuels [4]. However, the extraction of water consumes the majority of the energy required for ethanol production [5,6]. Wet ethanol, however, can fulfill this role, especially when it has more than 5% water (v/v), which leads to a reduction in production costs in the distillation process [7,8]. Gainey et al. also stated that wet ethanol is an interesting renewable fuel because of its potential to save the energy obtained through its production [9].

Multiple approaches to controlling gas emissions have been developed in recent decades, such as the reduction in engine volumes and the use of compressors ('downsizing') that allow a reduction in consumption without decreasing engine performance, as well as replacing fossil fuels with renewable fuels, such as ethanol [10]. This fuel, when hydrated, demands a greater amount of energy to change its physical state to the vapor phase. Water, for example, requires 2.26 MJ kg^{-1} at 100 °C, whereas ethanol only requires 0.839 MJ kg^{-1} [11]. Because of this extra demand for vaporization energy, there is a tendency towards a reduced combustion temperature for fuels with greater hydration, causing the resistance to knocking to increase [12].

Gohn et al. [13] carried out experiments to find out which hydrous ethanol mixture percentage optimized the combustion properties under operating conditions in a TSCI engine, whether it is naturally aspirated or supercharged. The authors tested four different mixtures and concluded that the mixture that had 80% ethanol and 20% water, based on mass, presented better combustion characteristics with respect to the inlet temperature, combustion efficiency, and thermal efficiency, regardless of the supercharging level. The addition of water with ethanol increases the specific mass of the fuel and reduces the temperature of the mixture and, consequently, the combustion chamber temperature. Research in the literature confirms that the engine under study is capable of operating with wet ethanol mixtures with up to 47% distilled water.

A study [14] testing four concentrations of distilled water (ranging from 10 to 40%) evaluated two engine conditions: (a) fixed ignition timing and (b) adjusted timing for maximum torque. The 30% distilled water mixture yielded the best results for power, torque, efficiency, specific fuel consumption, and lower exhaust gas temperatures. Mathematical and experimental models were developed to predict the performance of wet ethanol in internal combustion engines with a 12:1 volumetric compression ratio, showing relative errors below 13% across all tests. Additionally, the study observed a gradual increase in specific fuel consumption as the water content increased.

El-Seesy et al. [15] studied the injection of pure ethanol and wet ethanol into a diesel engine. The authors observed that the increase in the ethanol injection period leads to a reduction in the amount of ethanol entering the combustion chamber; the ignition delay increases with an increase in the water content in the aqueous ethanol solution.

Boldaji et al. [16] developed and validated a three-dimensional numerical model to investigate the use of the latent heat of vaporization of wet ethanol and to introduce the forced thermal stratification of thermally stratified compression ignition (TSCI), allowing control of the combustion process. The results showed that a higher percentage of water reduces the peak heat release rate and extends the combustion period.

Using flow and combustion visualization techniques, Koupaie et al. [17] carried out studies to verify the influence of the hydration content of fuels on flame propagation and the interaction of the internal flow during the combustion process. In the image analysis, it was observed that the flame propagation trend was towards the hottest regions of the combustion chamber. On the other hand, the presence of water increased the flame distortion resistance when compared to pure ethanol (iso-octane) and reduced the flame propagation velocity when the hydration increased. The authors suggested that the spark plug be tilted towards the inlet valve to create a more uniform flame front.

Based on exergy analysis, Trivedi and Haleem [18] evaluated the performance of an HCCI combustion engine using wet ethanol. The results were obtained by varying the efficiency of the exchanger/regenerator used as a source of heat to fire up the gasses from the turbocharger. Experiments were carried out using an engine with a 16:1 volumetric compression ratio and wet ethanol (35%) as fuel, with a variation in the efficiency of the regenerator between 75% and 83%. The results indicated the engine's combustion reactions as the maximum exergy destruction, followed by the catalytic converter caused by the chemical destruction of exergy.

Lanzanova et al. studied the use of ethanol with volumetric contents of distilled water between 5% and 40% on an engine converted from a diesel engine to one that operates in

the Otto cycle, with a volumetric compression ratio of 12:1. The analysis of the heat release, with the help of computational simulations, showed that the brake thermal efficiency remains nearly unchanged for mixtures of up to 30% v/v of distilled water [19].

In another study, Fagundez et al. evaluated the energy efficiency of wet ethanol (sub-azeotropic hydrated ethanol) in an engine with a volumetric compression ratio of 12:1. The authors proposed a new metric, based on the net energy factor, to calculate the efficiencies of moist and hydrous ethanol. The authors identified that the optimal efficiency was obtained with 70% (v/v) ethanol [20].

Sari et al. explored the optimal operating conditions for wet ethanol use in spark ignition engines with high compression rates. Ethanol–water fuel blends containing 4%, 10%, 20%, and 30% v/v of water in ethanol were tested and compared in engine tests, with three different compression rates (12.5, 13.5, and 14.5:1). The results showed that E80W20 is an optimum blend for increased engine efficiency and similar emissions of those of E4W96 while reducing fuel production costs [21].

Zapata-Mina et al. performed an exergetic analysis of a diesel engine with an original compression rate of 17:1 that had been converted to ignite while operating with diesel, ethanol (E100), and gasoline/ethanol blends with 10% (E10) and 50% (E50) of ethanol in mixture. The results indicate that the highest exergetic efficiency of 16.46% was achieved with E100 at a 9:1 compression ratio and a rotational speed of 2100 rpm, while the lowest efficiency of 9.6% was observed with diesel at a speed of 3200 rpm. Additionally, it was noted that a 12:1 compression ratio was advantageous for E50 and E10, though it had a negative impact on E100 under certain operating conditions. When running on diesel fuel, the engine displayed lower performance compared to when operating with E100, E50, or E10. This is due to variations in combustion temperature and, to a significant extent, the engine degradation caused by the chemical properties of E100 and its blends [22].

In a numerical comparative study, Li et al. evaluated the use of methanol, ethanol, and methane in a four-cylinder engine converted from a CI diesel engine to an SI engine with a compression ratio of 17.5, using a 1D simulation platform. Methane showed a lower heat release rate (HRR) compared to methanol and ethanol, as alcohols are oxygenated fuels and methanol contains up to 50% oxygen, which is more conducive to complete combustion. Equivalence ratios of 1.0 demonstrated the highest HRR, theoretically indicating complete combustion. When the engine operated at a low speed (800 rpm), the volumetric efficiency of ethanol was slightly higher than that of methanol and methane and nearly the same at 1600 and 2400 rpm. Ethanol also presented a higher maximum temperature than methane and methanol at almost all engine speeds and equivalence ratios. On the other hand, ethanol showed higher CO_2 emissions than the other fuels [23].

De Morais et al. converted a diesel generator to operate in the Otto cycle using ethanol as fuel, maintaining the original compression ratio of 17:1. In the diesel cycle, the engine was fueled with B7 diesel (diesel oil with 8% of biodiesel, and pure hydrous ethanol (ethanol with 4.9% of water) was used in Otto cycle. The greater resistance to the knocking effects of ethanol allows the use of higher volumetric compression ratio values, even in the presence of gasoline. The results indicated similar THC emissions between cycles, but increased CO_2, CO, and NO_x emissions in the Otto cycle with ethanol [12].

As presented above, there is a lack of studies in the literature investigating the use of ethanol in compression ignition (CI) engines converted to spark ignition (SI), especially under high compression ratios. Furthermore, there is a significant gap in understanding the effects of using wet ethanol with high water concentrations. The present work aims to study the performance and emissions of an Otto cycle power generator operating with wet ethanol containing high water concentrations of 7%, 17%, 27%, 37%, and 47% at a high volumetric compression ratio of 17:1.

2. Materials and Methods

To evaluate the performance and emissions of the tested fuels, and MWM 229-4(Brazil) engine, originally designed for the diesel cycle, was used. This engine was coupled to a

generator used to apply the load to the engine. A 50 kW resistive load bank was employed to convert power into heat and maintain the engine load. The characteristics of the test engine and generator are presented in Table 1, and Figure 1 illustrates the experimental apparatus.

Table 1. Test engine and generator details.

Equipment	Parameter	Type of Value
Engine	Cycle	Four stroke
	Injection	Port Fuel Injection
	Bore × stroke	102 × 120 mm
	Number of cylinders	4, in-line
	Compression ratio	17:1
	Total displacement	3922 cm^3
	Intake system	Naturally aspirated
Generator	Rated power	44.0 kW
	Number of poles	4
	Voltage	220 V
	Number of phases	3
	Rated power	55 kvA
	Frequency	60 Hz

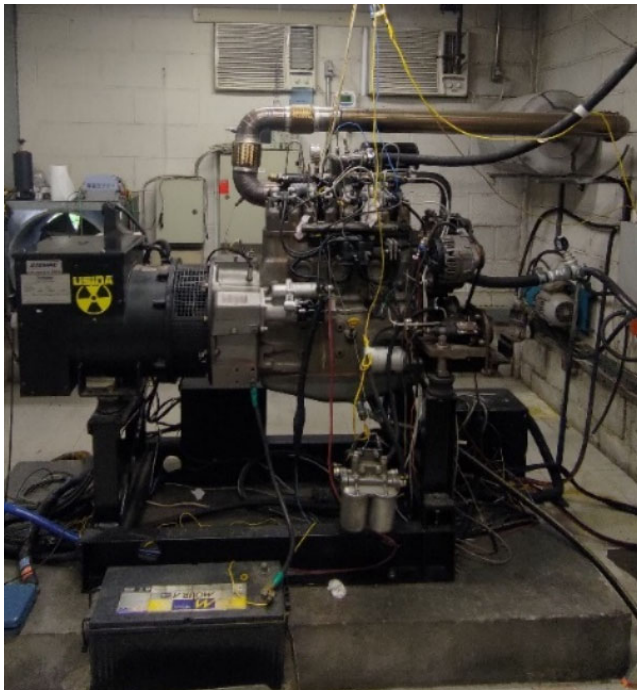


Figure 1. Experimental apparatus.

The engine was modified to operate on the Otto cycle while maintaining the original volumetric compression ratio of 17:1 [12]. Figure 2 shows a diagram of the experimental test bench used in the tests.

In Otto cycle engines, the amount of air admitted is controlled by a butterfly valve that operates according to the required power demand. Considering an increase in this demand, a greater amount of air is admitted and, consequently, more fuel is injected [12]. The injection system consisted of four PFI injectors located in the intake manifold, around 100 mm away from the valve seat. Therefore, it is important to highlight that the engine used to evaluate wet ethanol was equipped with an autonomous control system for positioning the butterfly valve that maintained a constant operating rpm on the engine (1800 ± 20 rpm) [24].

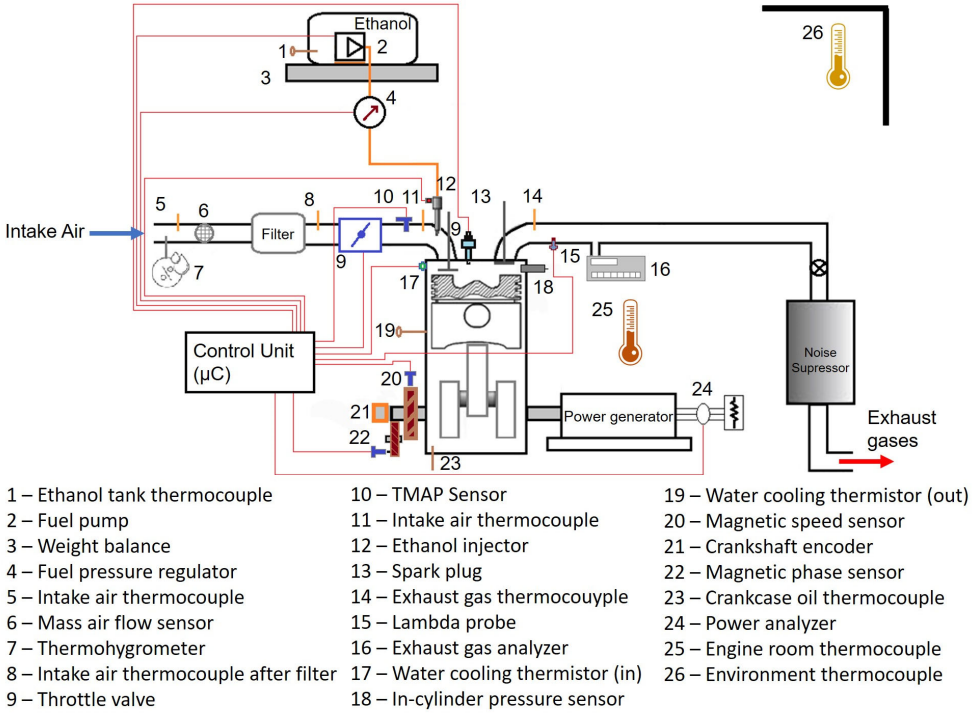


Figure 2. Schematic of the experimental bench.

The acquisition of experimental engine performance data was developed in LabView software (2018 version) [12]. To measure THC, NO_x, and CO emissions, with resolutions of ± 1 ppm and CO_2 emissions with a resolution of $\pm 0.01\%$, a gas analyzer (California Analytical Instruments, Orange, CA, USA) was integrated into the system. The engine was operated with a stoichiometric mixture.

In the tests, wet ethanol with 7% distilled water was used as the standard fuel. Higher hydration percentages were achieved through the addition of distilled water to the standard ethanol [12]. The hydration percentages (based on w/w) used in the tests were 7% (E93W07), 17% (E83W17), 27% (E73W27), 37% (E63W37), and 47% (E53E47) distilled water. The fuel's energy can be obtained through the product of its mass and its calorific power. In the burning of hydrogenated fuels, combustion gasses and steam are produced. This energy must be subtracted from the calorific value [12]. This procedure adopted the determination of the lower heating value (LHV) of each fuel used in the tests. A heat of vaporization of water of 2.44 MJ kg^{-1} was considered, and the values of the higher heating value (HHV) of each fuel were obtained. Table 2 presents the classification of the tested fuels with their respective LHV values and air/fuel (A/F) relations, calculated stoichiometrically.

Table 2. Fuel classification and LHV.

	Composition (*v*/*v*)		**Specification**	
	Ethanol	**H_2O**	**LHV**	**A/F**
	[%]	**[%]**	**[kJ/kg]**	**[-]**
E93W7	93	7	24.9	8.2
E83W17	83	17	21.7	7.2
E73W27	73	27	18.6	6.2
E63W37	63	37	15.9	5.2
E53W47	53	47	13.0	4.3

A problem arising from running an engine is the knocking effects that occur due to the appearance of disordered pressure peaks inside the combustion chamber, caused by the auto-ignition of the air/fuel mixture before the flame front [8,9,25]. It is possible to vary the

knocking intensity by controlling the ignition advance, since the intensity decreases as the ignition is slowed down, whereas it increases by advancing the ignition [26]. Considering this condition, and according to previous experiments, the initial value of the engine ignition angle was set at 13° BTDC. The ignition angle was configured for each load from the in-cylinder pressure curve analysis so that the engine operated without knocking. Ignition angle values for each of the fuels tested, according to its respective load, are shown in Table 3.

Table 3. Ignition angle (BTDC).

Load (kW)	E93W07	E83W17	E73W27	E63W37	E53W47
5.0	13°	13°	13°	13°	13°
10.0	13°	13°	13°	13°	13°
15.0	11°	13°	13°	13°	13°
20.0	11°	13°	13°	13°	13°
25.0	9°	11°	13°	13°	13°
27.5	8°	10°	13°	13°	13°
30.0	6°	9°	13°	13°	13°
32.5	5°	8°	13°	13°	13°
35.0	5°	7°	12°	13°	13°

The experimental procedure was carried out in accordance with the ISO guide 15550 [27]. The readings from each test were performed after the engine reached the steady-state condition and verified after the stabilization of the engine's rotation (1800 ± 20 rpm) and the cooling water's temperature (65 ± 1 °C).

For each fuel, four tests were conducted: two with increasing load sequences and two with decreasing load sequences. At each load level, the engine operated for a duration of two minutes in both directions. The detailed sequence of applied loads is presented in Table 4.

Table 4. Description of the test sequence.

Test	Load Coupling	A Sequence of Load [kW]
Case 1	Increasing	5.0–10.0–15.0–20.0–25.0–27.5–30.0–32.5–35.0
Case 2	Decreasing	35.0–32.5–30.0–27.5–25.0–20.0–15.0–10.0–5.0
Case 3	Increasing	5.0–10.0–15.0–20.0–25.0–27.5–30.0–32.5–35.0
Case 4	Decreasing	35.0–32.5–30.0–27.5–25.0–20.0–15.0–10.0–5.0

The load power, fuel consumption, and emission results were corrected to standard conditions for temperature and pressure. The total uncertainty of the results presented is a combination of both the instrument uncertainty and the statistical spread. Table 5 presents the characteristics of the measuring instruments shown in Figure 2.

The uncertainties in the experiments were calculated by considering the uncertainties of the equipment and measurements. The Kline and McClintock [28] method was used to calculate the combined uncertainty (w_R), as shown in Equation (1).

$$w_R = \left[\left(\frac{\partial R}{\partial x_1} w_1 \right)^2 + \left(\frac{\partial R}{\partial x_2} w_2 \right)^2 + \left(\frac{\partial R}{\partial x_n} w_n \right)^2 \right]^{1/2} \quad (1)$$

R = fictional parameter R, which is a function of two or more variables (x_1, x_2,... x_n);

w_1, w_2, and w_n = independent uncertainty variables [dimensionless];

$\partial R/(\partial x_1)$, $\partial R/(\partial x_2)$, and $\partial R/(\partial x_n)$ = partial derivative of the result R in function of the independent variables [dimensionless].

The combined uncertainty incorporates both Type A and Type B uncertainties. Type A uncertainty is determined by the statistical distribution of values obtained through repeated

measurements, while Type B uncertainty arises from systematic sources of error in the measurement process, such as equipment-related uncertainties in this study. Parameters like CO, CO_2, NO_x, and THC emission rates are measured using a single piece of equipment, simplifying Equation (1). In contrast, parameters such as intake air mass flow rate, specific fuel consumption, and fuel conversion efficiency involve multiple variables and equipment, with their formulation adhering to Equation (1).

Finally, the expanded uncertainty of a parameter R (I_R) is calculated by multiplying by Student's *t* coefficient. In this study, the effective degrees of freedom are assumed to be infinite, resulting in a Student's *t* coefficient of 2 for a 95.4% confidence level, as described by Equation (2).

$$I_R = w_R \cdot t \quad (2)$$

Table 5. Instrumentation characteristics.

Measurement Variable	Instrument	Measuring Range	Uncertainty
Fuel temperature	Pt-100 CONSISTC, SÃO PAULO, BRAZIL	0 to 40 °C	±0.35%
Cooling temperature	Pt-100	0 to 150 °C	±0.35%
Inlet air temperature	Thermocouple type K CONSISTC, SÃO PAULO, BRAZIL	0 to 40 °C	±0.4%
Ambient temperature	Thermocouple type K	0 to 40 °C	±0.4%
Oil temperature	Thermocouple typgtge K	0 to 40 °C	±0.4%
Exhaust gas temperature	Thermocouple type K	0 to 700 °C	±0.4%
Relative humidity	KIMO HTP300 KIMO—EMERAINVILLE—FRANÇA	0 to 100% U.R.	±1.5%
Atmospheric pressure	KIMO HTP300	0 to 2000 mbar	±1 mbar
Electrical power	Cyber UPD-200 ENGELETRICA—SÃO PAULO—BRAZIL	0 to 300 kW	±1.0%
Air mass flow	Bosch HFM-4.7 RP BOSCH—GERLINGEN—ALEMANHA	10 to 620 kg/h	±1.0%
Fuel mass	Líder LD1050	0 to 50 kg	±1.0 g
Crankshaft angle	Dynapar B58N DYNAPAR—SÃO PAULO—BRAZIL BOSCH—GERLINGEN—ALEMANHA	max. 6000 rpm	±0.5°
Combustion chamber pressure	Kislter 6061B KISTER—WINTERTHUR—SUÍÇA	0 to 250 bar	Linearity: ±0.5% FSO
NO_x emission	CAl 600-HCLD CAl 600-HCLD—CALIFORNIA ANALYTICAL INSTRUMENTS—ORANGE—USA	0 to 3000 ppm	Linearity and Repetitiveness: ±0.5% FSO
THC emission	CAl 600-MHFID CALIFORNIA ANALYTICAL INSTRUMENTS—ORANGE—USA	0 to 30,000 ppm	
CO_2, CO, and O_2 emission	CAl 600-NDIR CALIFORNIA ANALYTICAL INSTRUMENTS—ORANGE—USA	0 a 100%	Linearity:±0.5% FSORepetitiveness: ±1.0% FSO

3. Results and Discussion

This section presents the results obtained and discusses the performance and emissions of the engine studied, with a volumetric compression ratio of 17:1 and the indirect injection of wet ethanol with 7%, 17%, 27%, 37%, and 47% (*w*/*w*) distilled water. The injection timing for the port fuel injectors running a stratified charge was kept constant throughout the tests. The start of the injections was always 0°, referenced from the intake top dead center. Spark timing was adjusted to keep the engine at maximum brake torque unless the combustion knock limit was reached first. The main variables analyzed were the specific fuel consumption, the air mass flow, the pressure in the combustion chamber, the heat release rate, the exhaust gas temperature, emissions, and the brake thermal efficiency.

3.1. Specific Fuel Consumption

The mass of the fuel tank, measured before and after the tests, was adopted as a parameter for controlling the specific fuel consumption (SFC) of the engine. The SFC is used to compare internal combustion engines, as it makes it possible to measure the flow of fuel per unit of power. To compute the specific consumption of each fuel, the value subtracted from the distilled water mass was adopted, leaving out the mass of pure ethanol consumed, regarding the load applied to the engine. When applied in the analysis of the results, this methodology shows the distilled water's impact on the operation of the engine tested. Figure 3 shows the SFC calculation, disregarding the different percentages of the distilled water present in the ethanol mixture as a function of the applied loads. As expected, specific fuel consumption decreased with the increasing load across all tests. The decreasing behavior of this parameter, as the load increases, is caused by the addition of power to a constant rpm [12]. The maximum absolute uncertainty is 0.0152 kg/kWh, as shown at the 5 kW load for fuel E83W17.

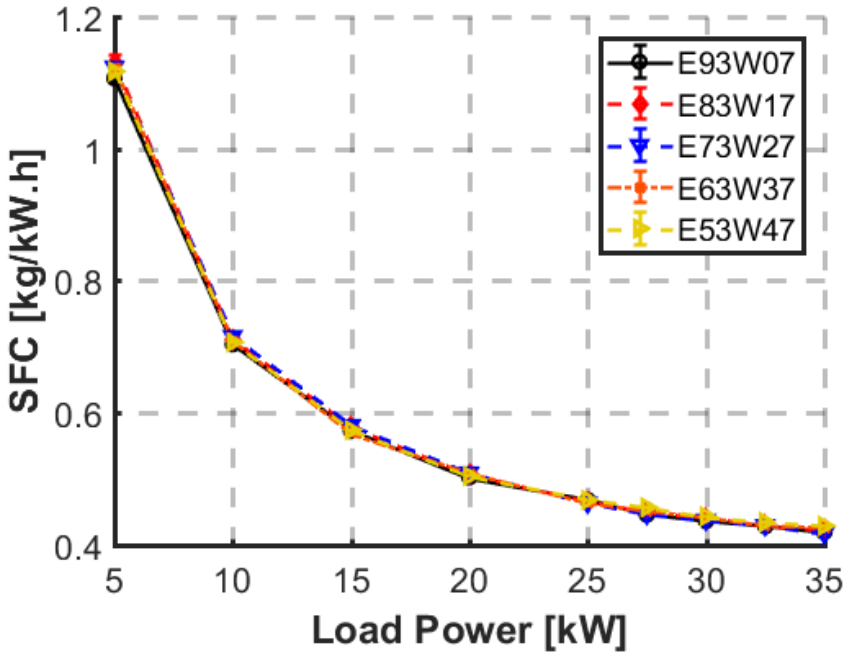


Figure 3. SFC of ethanol fuel.

Through Figure 3, it is possible to conclude that there were no significant variations in ethanol consumption, regardless of the volume of distilled water in each of the fuels analyzed. Similar results of SFC were discussed by [12], who used the same engine in the Otto cycle. However, in this work, the fixed ignition angle (6° BTDC) without wet ethanol (E93W07) was used and equipped with a different engine control system.

3.2. Air Mass Flow

The behavior of the air mass flow admitted into the engine, depending on the load applied to each experiment, is shown in Figure 4. It was observed that the air mass flow values corresponding to the power demand showed no significant variations, regardless of the hydration percentages experienced. This behavior was already expected since the results of SFC also did not show significant variations. The maximum absolute uncertainty is 5.64 kg/h shown at the 35 kW load for fuel E73W27.

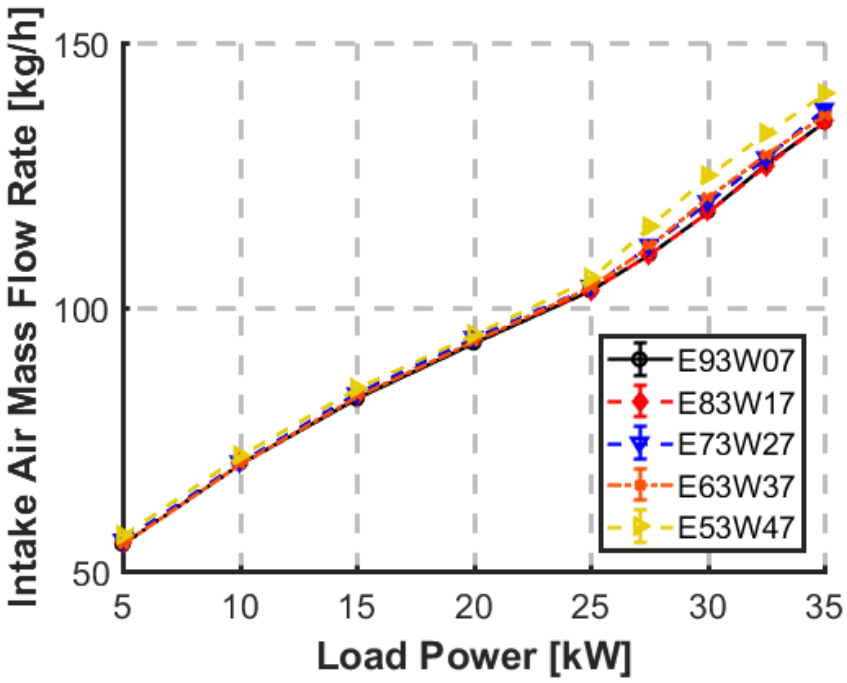


Figure 4. Mass flow rate versus load power.

3.3. Pressure and Heat Release Rate

According to [26], the heat release rate increases after the ignition of the air/fuel mixture. In the sequence, the value tends towards zero at the end of the combustion. Three load positions were chosen: the first at a low load (5.0 kW), the second at an intermediate load (27.5 kW), and the last at a higher load (35.0 kW). Figure 5 shows the pressure inside the cylinder (a) and the heat release (b) for all fuels analyzed at a load of 5.0 kW. The data displayed in Figure 5 represent the average results from a single cylinder over 200 combustion cycles. For this load, the highest pressure peak value was 24 bar at 10° ATDC, operating with E73W27, and the smallest pressure peak was 19 bar at 15° ATDC, operating with E53W47.

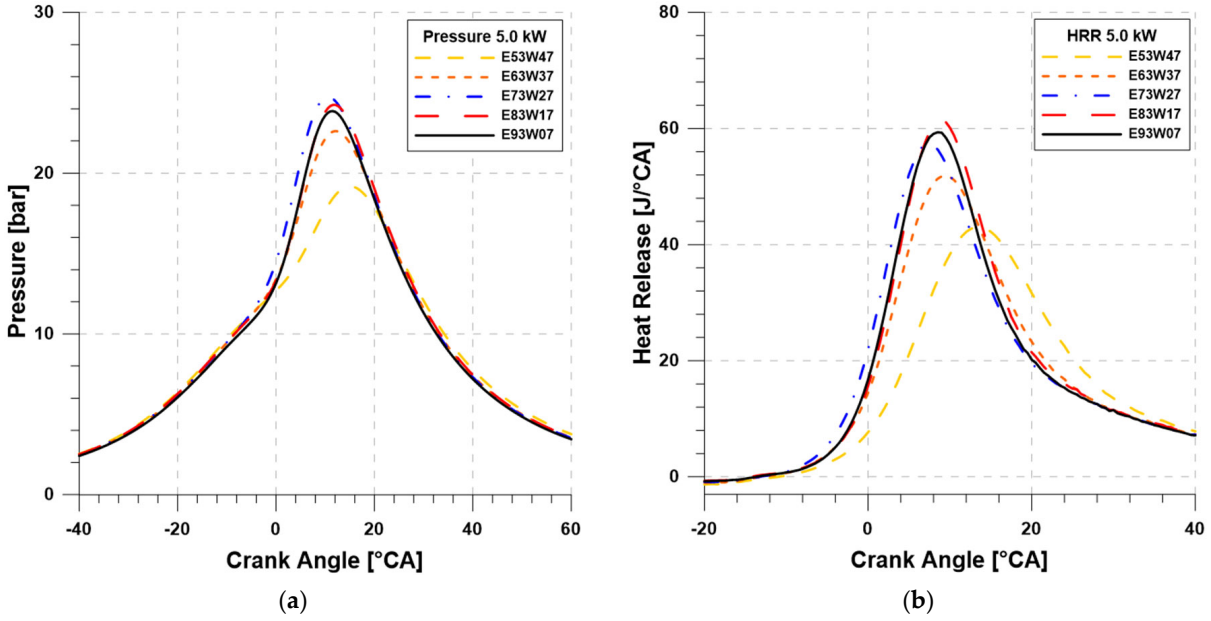
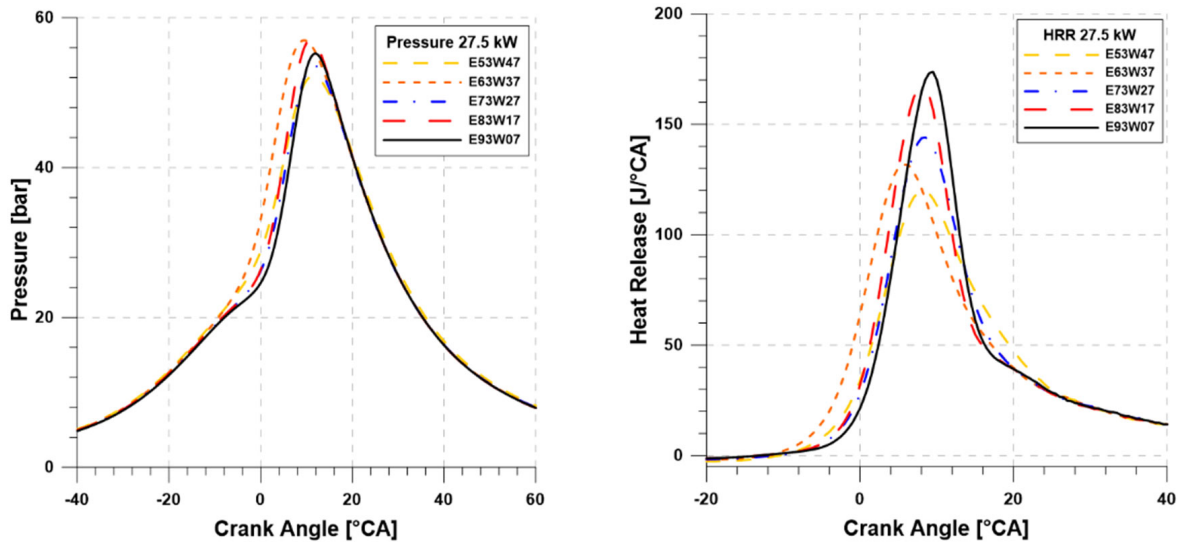


Figure 5. Internal pressure and heat release rate for a 5.0 kW load. (**a**) Cylinder internal pressure. (**b**) Heat release rate.

A trend of reducing maximum heat release rate is observed when operating with a 5 kW load and when the distilled water content of the fuel increases. This is explained because a greater amount of water mass requires a greater amount of energy to change its state from a liquid to a vapor. Part of the heat release rate is used to change the state of the water. Given the low engine load, the knock limit was not a limiting factor; the engine was running at maximum brake torque, regarding spark timing efficiency. In this specific operating load point, the usage of hydration did not yield better brake thermal efficiency or an improvement in performance.

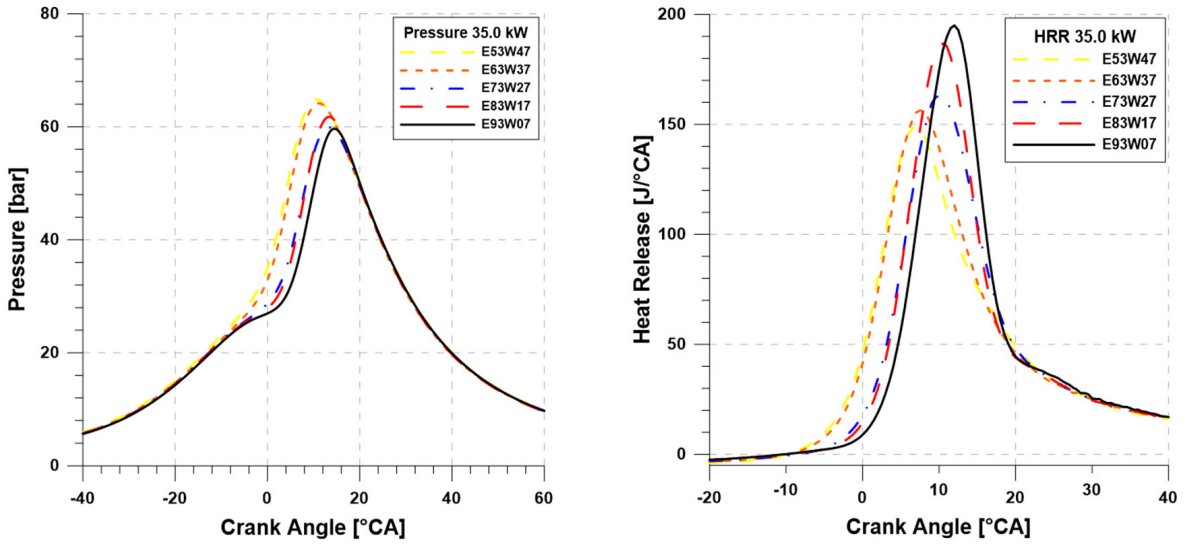
Figure 6 shows the pressure inside the cylinder (a) and the heat release (b) for all blends of fuels analyzed at a load of 27.5 kW. For this load, the highest peak pressure value was 57 bar at 10° ATDC, operating with both E83W17 and E63W37. The smallest value was 52 bar at 12° ATDC, operating with E53W47. It should be noted that the pressure peaks were greater than for the 5.0 kW load. This phenomenon can be explained by the greater demand for power, which makes the engine admit more air and inject more fuel, increasing the power generated. With this load, and with the increase in the hydration of the ethanol, the peaks in the heat release rate and temperature inside the cylinder tend to decrease as the water content in the fuel increases. This phenomenon can be justified by the increase in the latent heat caused by the reduction in the ethanol content in the blend.



(**a**) (**b**)

Figure 6. Internal pressure and heat release rate for a 27.5 kW load. (**a**) Cylinder internal pressure. (**b**) Heat release rate.

Figure 7 shows the pressure inside the cylinder (a) and the heat release (b) for all blends analyzed at a load of 35.0 kW. The highest pressure peak of 69 bar for this load occurred when the engine was operated with E53W47 at 11° ATDC. The lowest pressure peak was 60 bar at 16° ATDC, operating with E93W07, E83W17, and E73W2. The higher pressure peaks during the combustion of fuel blends with higher water/ethanol ratios are due to the incompressible nature of water and the increased total fuel mass required to maintain the same ethanol/air ratio, which results in higher compression pressures prior to combustion heat release. The lower heat release rates observed with higher water/ethanol ratios can be explained by the heat loss caused by water vaporization, which extracts heat from the mixture.



(**a**) (**b**)

Figure 7. Internal pressure and heat release rate for a 35.0 kW load. (**a**) Cylinder internal pressure. (**b**) Heat release rate.

The pistons perform greater compression work, increasing the pressure in the combustion chamber. For the 35.0 kW load, it was possible to observe the same behavior of the heat release rate inside the cylinder when the engine was operated at both 5.0 kW and 27.5 kW loads. With this load, a reduction in the heat release rate peak is seen, with an increase in the water content in the fuel. Since it is a high load, a large amount of fuel is injected into the engine and the amount of energy needed for the water from the injected fuel to evaporate is higher. As it is an endothermic process, this action reduces the peaks of the heat release rate. The increase in the degree of hydration of the ethanol allowed the engine to operate with higher ignition angle advances, allowing the engine to work without the detonation phenomenon for the entire applied load range for all tested fuels. This fact shows that water functions as an anti-knocking additive.

The analysis of the results across different load conditions reveals a trend: the addition of water to ethanol reduces the heat release rate. This reduction is attributed to the energy required for the evaporation of the additional water. In terms of pressure, a trend is observed at higher loads, where the addition of water to ethanol increases the peak cylinder pressure. This is due to the greater ignition advance compared to standard ethanol (E93W07) and the increased mass inside the cylinder.

3.4. Ignition Delay

Through its enthalpy of vaporization, water absorbs heat from the combustion chamber during both the compression and expansion processes of the mixture admitted during the intake cycle. The hydration of ethanol fuel lowers the combustion chamber temperature because water extracts heat from the mixture. The lower temperature in the combustion chamber allows the engine to operate with more advanced spark timing, shifting the MFB 50 closer to MBT.

Lowering the temperature of the combustion chamber relates directly to lower energy levels within the combustion chamber prior to the spark. Lowering the overall energy levels within the combustion chamber directly affects the time necessary to reach the ignition of the mixture and is related to the moment at which the spark is applied. The relationship between spark timing and the start of combustion (SOC) is shown in Figure 8 as the ignition delay. It is evident from Figure 8 that higher levels of ethanol hydration cause a longer ignition delay. Comparing 37% to 7% hydration shows an increase of 6° in ignition delay, slowing down the start of combustion. In order to keep the MFB 50 of the initial hydration

level, the spark timing was advanced due to the longer ignition delay and lower knocking sensitivity.

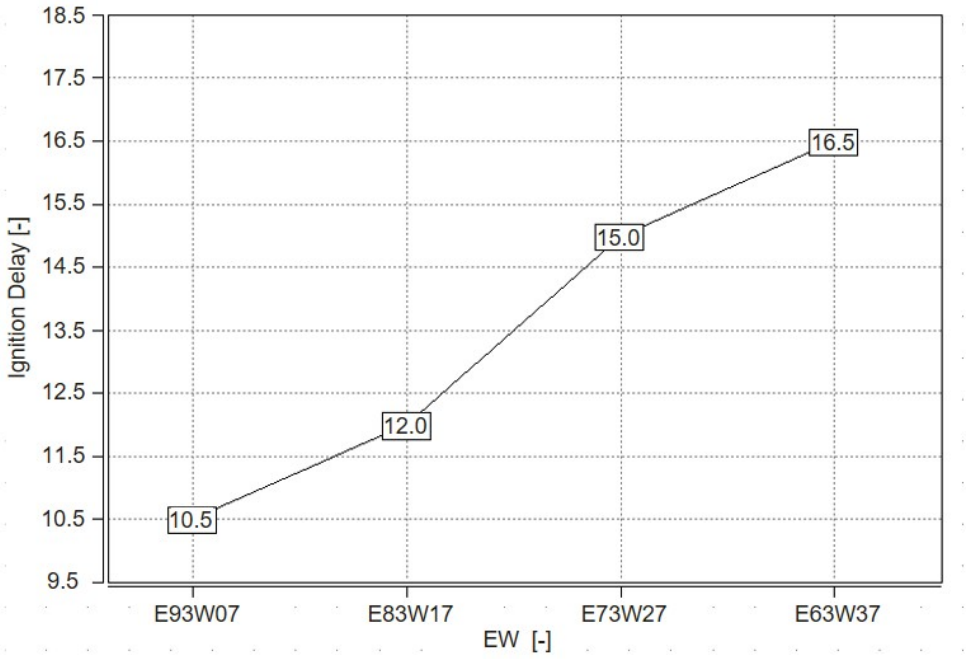


Figure 8. Ignition delay.

3.5. Exhaust Temperature

Engine fuel consumption is directly influenced by the power demand on the shaft. Larger loads require greater burning of fuel, which promotes a greater release of energy and, therefore, increases the exhaust temperature. In faster combustion, a decrease in the exhaust temperature can be seen [26]. Considering the fuels (the base is ethanol and the rest is distilled water), one can say that no change in the combustion kinetics happened. Table 6 shows the exhaust temperatures for each of the fuels tested, depending on the load, with an uncertainty of ±6.86%.

Table 6. Exhaust gas temperature for different engine power loads and fuels.

	Load [kW]	**5.0**	**10.0**	**15.0**	**20.0**	**25.0**	**27.5**	**30.0**	**32.5**	**35.0**
					Exhaust temperature [°C]					
Fuel	E93W07	499	520	540	556	577	592	603	611	615
	E83W17	481	481	543	543	567	581	592	608	601
	E73W27	476	500	537	537	558	574	587	596	602
	E63W37	472	495	532	532	550	561	569	579	586
	E53W47	473	493	528	528	544	554	561	567	571

There is a tendency for the exhaust gas temperature to decrease as the ethanol hydration increases, which is due to the energy consumed in the water vaporization process [12,14,21]. The highest temperature for the maximum load of 35.0 kW was 615 °C when using E93W07 fuel, and the lowest temperature was 571 °C when using E53W47. This represents a 7% decrease in temperature.

3.6. Specific CO_2, CO, THC, and NO_x Emissions

The burning of hydrocarbons, such as ethanol, is a reduction–oxidation process that releases energy and has carbon dioxide (CO_2) as its product. The emission of this gas by internal combustion engines is directly correlated with the amount of fuel consumed and

the combustion quality [29,30]. Figure 9 shows the behavior of the specific CO_2 emissions of the fuels tested, according to the load applied. It can be seen that CO_2 emissions are not influenced by the distilled water in the fuels. As expected, specific CO_2 emissions decreased with increasing loads across all tests. This behavior can be explained by the SFC, in which equivalent products of CO_2 are expected for the same amount of burned ethanol.

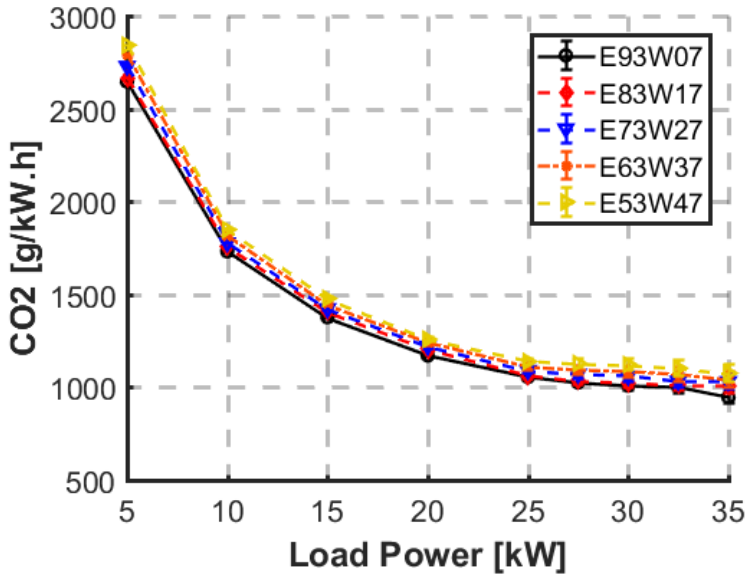


Figure 9. Specific CO_2 emissions.

A product of the incomplete combustion of hydrocarbons is carbon monoxide (CO), whose formation is increased by the high temperatures inside the combustion chamber [26,30]. Figure 10 shows the specific emission of CO as a function of the load applied to the different hydrations of ethanol. As expected, specific CO emissions decreased with increasing load across all tests. The tendency observed for CO emissions is to decrease as the percentage of distilled water in ethanol increases. This behavior can be correlated with the reduction in the temperature of the exhaust gasses, which highlights lower temperatures in the combustion chamber and avoids the formation of CO. When comparing the emissions of E93W07 and E53W47 fuels, there was a maximum reduction of 43% and 56% at loads of 5.0 and 35.0 kW, respectively [12].

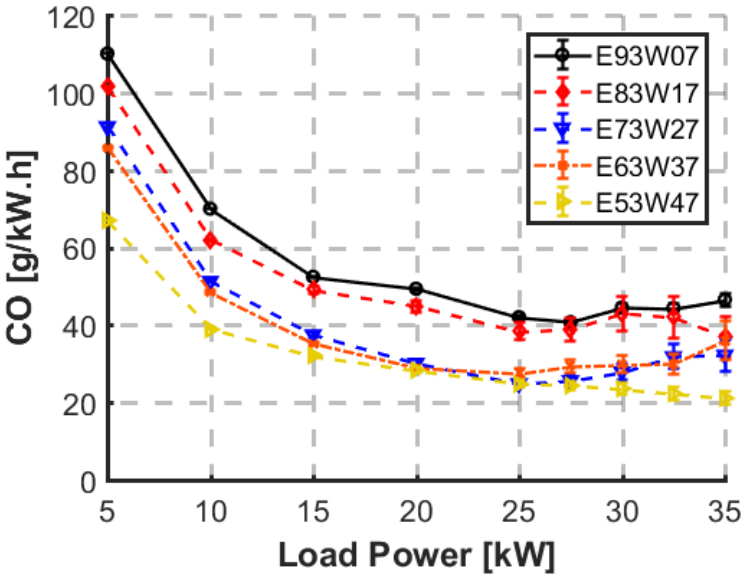


Figure 10. Specific CO emissions.

Another parameter which is used to assess the quality of combustion in engines is the quantification of emissions of unburned hydrocarbons (THC). The inherent characteristics of the combustion process, such as the incomplete burning of fuels, low temperature in the combustion chamber, and fuel containment, increase THC emissions [8]. Figure 11 shows the values of THC emissions for each fuel tested at each applied load. As expected, specific THC emissions decreased with increasing loads across all tests. It can be seen that increasing the percentage of distilled water in the fuel increases THC emissions.

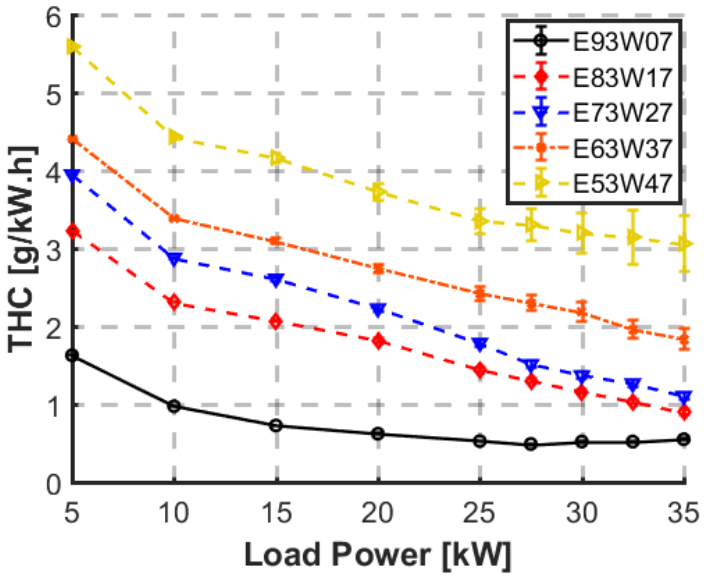


Figure 11. Specific THC emissions.

Based on the SFC and CO_2 emission results, which do not show an increase as the percentage of distilled water in the mixture increases, besides CO reduction, it can be said that this increase in THC emissions is not related to a loss of combustion quality. The increase in both SFC and CO, as well as the reduction in CO_2, would directly impact THC. This result may be related to a lower temperature in the combustion chamber and a larger quantity of distilled water inside the cylinder, which makes the containment of fuel in cracks easier. The results in [21] were similar to those found in this work. However, [12] reported THC emission behavior close to that measured using the engine used in this work but while operating in the diesel cycle.

Emissions of nitrogen oxides (NO_x) represent emissions of nitric oxide (NO) and nitrogen dioxide (NO_2), which are harmful to humans. In internal combustion engines, the formation of NO_x is mostly influenced by temperature and pressure in the combustion chamber [26,31]. NO_x formation is considered insignificant at temperatures below 1800 K. The mechanism of Zeldovich [32] best describes the formation of these gasses in engines that operate with air/fuel mixtures close to the stoichiometric.

Figure 12 shows the specific emissions of NO_x for each fuel tested, depending on the applied load of the motor shaft. The tendency towards the reduction in NO_x emissions, associated with the increase in the percentage of distilled water present in the fuel, was notable. This behavior is evident in the curves of the engine's specific NO_x emissions when operating with E63W37 and, mainly, E53W47 fuels, with the latter showing reductions of 23–80% compared with the standard fuel, E93W07.

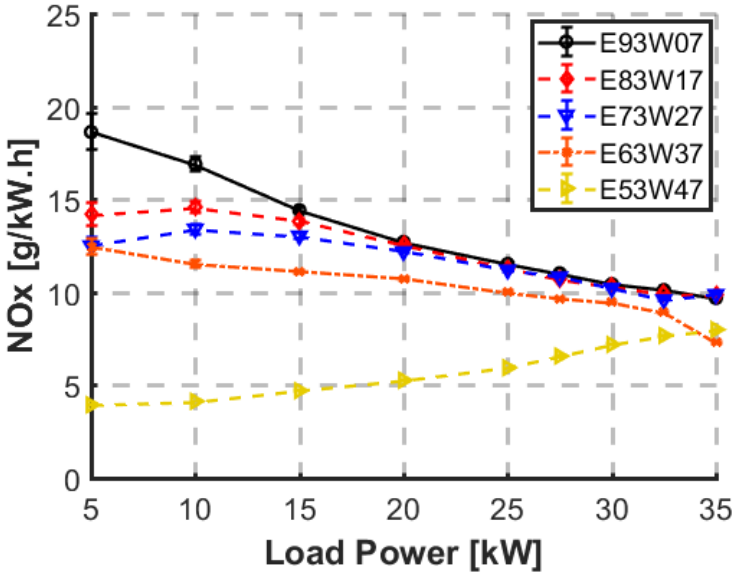


Figure 12. Specific NO_x emissions.

The reduction in exhaust gas temperatures, which is associated with an increase in THC and, therefore, associated with an increase in distilled water in ethanol, suggests a decrease in temperature in the combustion chamber. Since NO_x formation is directly affected by temperature, this result is a consequence of the lower temperatures in the combustion chamber, which are caused by the energy used in the vaporization of the distilled water in the fuel. Reference [12] reported reductions in NO_x emissions related to the overhydration of ethanol in their work.

The 37.5 kW load showed the highest uncertainties for the emissions index, with values close to 5%.

3.7. Brake Thermal Efficiency

The brake thermal efficiency is the relationship between the power generated by the engine and the product between the lower calorific value (PCI) and the fuel mass flow. Fuel conversion efficiency was calculated by considering the brake horsepower, which accounts for the combustion work provided, minus the compression work expended, as well as pumping and friction losses. Several factors can influence the brake thermal efficiency of an Otto cycle engine, including ignition timing and the physicochemical properties of the intake air and fuel [26].

Figure 13 presents the fuel conversion efficiencies for all proposed ethanol hydration percentages, based on the load applied to the engine shaft. The conversion efficiency values of the tested fuels remained similar and within the uncertainty ranges, with a maximum value of 33 $\pm$ 1% at a load of 35.0 kW. Based on the SFC results—a parameter whose variation has a significant impact on efficiency—the mass flow of admitted air, and CO_2 emissions, which were not notably influenced by the increase in the distilled water percentage, it is expected that brake thermal efficiency would remain unaffected. Experimental tests [14] indicate that ethanol fuel, even with hydration levels of up to 30%, can still perform efficiently. Sari [21] utilized an engine with a lower volumetric compression ratio than the one used in this study and reported a loss in brake thermal efficiency due to the increased distilled water content in the mixture. However, [12] reported efficiency gains with fuel hydration increases of up to 15%.

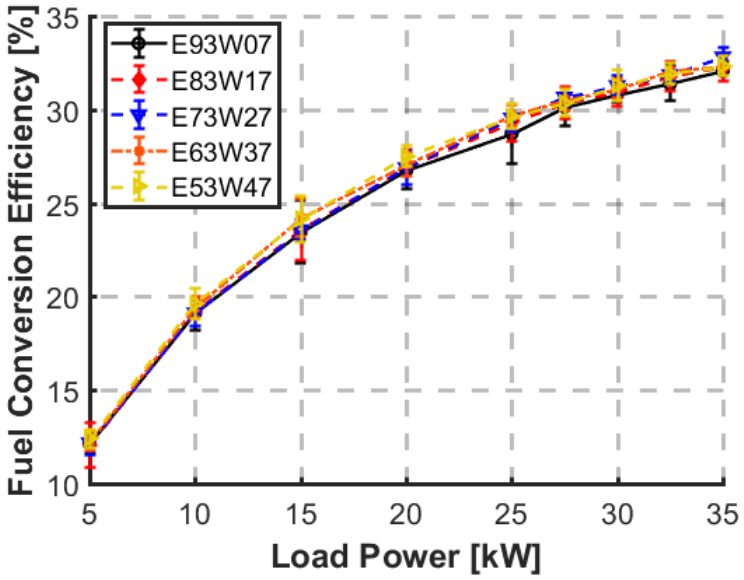


Figure 13. Fuel conversion efficiency.

4. Conclusions

The performance and emissions of a high-volumetric compression ratio engine (17:1), operating in the Otto cycle with hydrous ethanol (17%, 27%, 37%, and 47%), were assessed. The engine maintained steady operation across all load ranges and ethanol concentrations without detonation, indicating that higher ethanol hydration allowed for greater ignition advances. This was attributed to the cooler combustion chamber temperature resulting from water vaporization, which reduced the risk of detonation. The highest peak pressure occurred at a 35.0 kW load with E53W47 fuel, due to the increased fuel mass required to meet power demands. Fuel consumption increased with higher water content; however, the specific fuel consumption of pure ethanol showed minimal change. CO_2 emissions remained stable, while CO and NO_x emissions decreased, and THC emissions increased with higher ethanol hydration. This study demonstrates the feasibility of using hydrous ethanol in Otto engines, which could reduce fossil fuel dependency and promote renewable fuels, particularly for electricity generation. This study has limitations, such as the specific adaptation of the diesel-to-Otto cycle engine and the controlled laboratory conditions. Future research should explore varying operating conditions and long-term engine wear.

Author Contributions: Conceptualization, V.G.M.; Methodology, V.G.M., T.N., R.M.J. and C.B.M.; Formal analysis, B.E.P.F., R.M.J., H.J.J.d.S. and C.B.M.; Investigation, V.G.M. and T.N.; Writing—original draft, S.d.M.H., R.M.J. and H.J.J.d.S.; Supervision, S.d.M.H.; Project administration, S.d.M.H. All authors have read and agreed to the published version of the manuscript.

Funding: This research was supported by The Brazilian National Council for Scientific and Technological Development-CNPq, The Foundation of Research Support of the State of Minas Gerais-FAPEMIG, and The "Coordenação de Aperfeiçoamento de Pessoal de Nível Superior"-CAPES (Financial Code 001).

Data Availability Statement: The original contributions presented in this study are included in the article. Further inquiries can be directed to the corresponding author.

Conflicts of Interest: The authors declare no conflict of interest.

Nomenclature

A/F: air/fuel ratio
ATDC: after top dead center
BTDC: before top dead center
CA: crack angle
CO: carbon monoxide
CO_2: carbon dioxide
E93W07: ethanol with 7% m/m of distilled water
E83W17: ethanol with 17% m/m of distilled water
E73W27: ethanol with 27% m/m of distilled water
E63W37: ethanol with 37% m/m of distilled water
MBT: maximum brake torque
E53W47: ethanol with 47% m/m of distilled water
HCCI: homogeneous charge compression ignition
NO_x: nitrogen oxide
NO: nitric oxides
NO_2: nitrogen dioxide
LHV: lower heating value
HHV: higher heating value
SFC: specific fuel consumption
THC: hydrocarbon content
TSCI: thermally stratified compression ignition
MFB50: point of 50% of mass fraction burnt

References

1. United Nations. Framework Convention on Climate Change. *Paris Agreement*. 2015. Available online: https://unfccc.int/sites/default/files/english_paris_agreement.pdf (accessed on 1 November 2024).
2. Qasem, N.A.A.; Mourad, A.; Abderrahmane, A.; Said, Z.; Younis, O.; Guedri, K.; Kolsi, L. A recent review of aviation fuels and sustainable aviation fuels. *J. Therm. Anal. Calorim.* **2024**, *149*, 4287–4312. [CrossRef]
3. Bousbaa, H.; Kaid, N.; Alqahtani, S.; Maatki, C.; Naima, K.; Menni, Y.; Kolsi, L. Prediction and Simulation of Biodiesel Combustion in Diesel Engines: Evaluating Physicochemical Properties, Performance, and Emissions. *Fire* **2024**, *7*, 364. [CrossRef]
4. Feng, M.; Jiang, X.Z.; Zeng, W.; Luo, K.H.; Hellier, P. Ethanol oxidation with high water content: A reactive molecular dynamics simulation study. *Fuel* **2019**, *235*, 515–521. [CrossRef]
5. Feng, H.; Zhang, H.; Wei, J.; Li, B.; Wang, D. The influence of mixing ratio of low carbon mixed alcohols on knock combustion of spark ignition engines. *Fuel* **2019**, *240*, 339–348. [CrossRef]
6. Lama, L.G.; Sotton, J.; Martins, C.A. Experimental burning velocities of ethanol-water-air at elevated pressure and temperature. *Fuel* **2020**, *265*, 116933. [CrossRef]
7. Capellán-Pérez, I.; de Castro, C.; González, L.J.M. Dynamic energy return on energy investment (EROI) and material requirements in scenarios of global transition to renewable energies. *Energy Strategy Rev.* **2019**, *26*, 100399. [CrossRef]
8. Fagundez, J.L.S.; Sari, R.L.; Garcia, A.; Pereira, F.M.; Martins, M.E.S.; Salau, N.P.G. A chemical kinetics based investigation on laminar burning velocity and knock occurrence in a spark-ignition engine fueled with ethanol–water blends. *Fuel* **2020**, *280*, 118587. [CrossRef]
9. Gainey, B.; Gohn, J.; Hariharan, D.; Rahimi-Boldaji, M.; Lawler, B. Assessing the impact of injector included angle and piston geometry on thermally stratified compression ignition with wet ethanol. *Appl. Energy* **2020**, *262*, 114528. [CrossRef]
10. Bromberg, L.; Jo, Y.S.; Heywood, J. Optimal use of ethanol in dual fuel applications. *SAE Int. J. Engines* **2016**, *9*, 1087–1101.
11. Couper, J.R.; Penney, W.R.; Fair, J.R.; Walas, S.M. *Chemical Process Equipment: Selection and Design*, 2nd ed.; Gulf Professional Publishing: Houston, TX, USA, 2004.
12. De Morais, A.M.; Hanriot, S.M.; Oliveira, A.; Justino, M.A.; Valente, O.S.; Sodré, J. An assessment of fuel consumption and emissions from a diesel power generator converted to operate with ethanol. *Sustain. Energy Technol. Assess.* **2019**, *35*, 291–297. [CrossRef]
13. Gohn, J.; Gainey, B.; Zainul, S.; Lawler, B. Wet ethanol in LTC: How water fraction and DTBP affect combustion and intake temperature at naturally aspirated and boosted conditions. *Fuel* **2020**, *267*, 117094. [CrossRef]
14. Ambrós, W.M.; Lanzanova, T.D.M.; Fagundez, J.L.S.; Sari, R.L.; Pinheiro, D.K.; Martins, M.E.S.; Salau, N.P.G. Experimental analysis and modeling of internal combustion engine operating with wet ethanol. *Fuel* **2015**, *158*, 270–278. [CrossRef]
15. El-Seesy, A.I.; Kayatas, Z.; Takayama, R.; He, Z.; Kandasamy, S.; Kosaka, H. Combustion and emission characteristics of RCEM and common rail diesel engine working with diesel fuel and ethanol/hydrous ethanol injected in the intake and exhaust port: Assessment and comparison. *Energy Convers. Manag.* **2020**, *205*, 112453. [CrossRef]
16. Boldaji, M.R.; Gainey, B.; Lawler, B. Thermally stratified compression ignition enabled by wet ethanol with a split injection strategy: A CFD simulation study. *Appl. Energy* **2019**, *235*, 813–826. [CrossRef]
17. Koupaie, M.; Cairns, A.; Vafamehr, H.; Lanzanova, T. A study of hydrous ethanol combustion in an optical central direct injection spark ignition engine. *Appl. Energy* **2019**, *237*, 258–269. [CrossRef]
18. Trivedi, S.K.; Haleem, A. Thermodynamic analysis and utilization of wet ethanol in homogeneous charge compression ignition engine. *Int. J. Sustain. Energy* **2016**, *35*, 33–46. [CrossRef]

19. Lanzanova, T.D.; Vielmo, H.A.; Sari, R.L.; Dornelles, H.M.; Tatsch, G.A.; Martins, M.E.; Michels, L. *Performance Analysis of a Spark Ignited Engine Running on Different Water-in-Ethanol Mixtures*; SAE Technical Paper No. 2013-36-0202; SAE International: Warrendale, PA, USA, 2013.
20. Fagundez, J.L.S.; Sari, R.L.; Mayer, F.D.; Martins, M.E.S.; Salau, N.P.G. Determination of optimal wet ethanol composition as a fuel in spark ignition engine. *Appl. Therm. Eng.* **2017**, *112*, 317–325. [CrossRef]
21. Sari, R.L.; Golke, D.; Enzweiler, H.J.; Salau, N.P.G.; Pereira, F.M.; Martins, M.E.S. Exploring optimal operating conditions for wet ethanol use in spark ignition engines. *Appl. Therm. Eng.* **2018**, *138*, 523–533. [CrossRef]
22. Zapata-Mina, J.; Restrepo, A.; Romero, C.; Quintero, H. Exergy analysis of a diesel engine converted to spark ignition operating with diesel, ethanol, and gasoline/ethanol blends. *Sustain. Energy Technol. Assess.* **2020**, *42*, 100803. [CrossRef]
23. Li, X.; Zhen, X.; Xu, S.; Wang, Y.; Liu, D.; Tian, Z. Numerical comparative study on knocking combustion of high compression ratio spark ignition engine fueled with methanol, ethanol and methane based on detailed chemical kinetics. *Fuel* **2021**, *306*, 121615. [CrossRef]
24. Marques, R.B.D.T.; Faria, R.O.; Moreira, V.G.; Justino, M.A.M.; Valente, O.S.; Hanriot, S.M. *Engine Speed Control of a Diesel Power Generator Converted into Otto Cycle through Control of Inlet Air 2019*; Volume 5805 of LNCS; Springer: Berlin/Heidelberg, Germany, 2019; ISSN 2357-7592. [CrossRef]
25. Liu, L.; Zhang, Q. Comparison of detonation characteristics for typical binary blended fuel. *Fuel* **2020**, *268*, 117351. [CrossRef]
26. Heywood, J.B. *Internal Combustion Engine Fundamentals, xxxiv ed.*; McGraw-Hill: New York, NY, USA, 1988.
27. *ISO 15550:2016*; Internal Combustion Engines—Determination and Method for the Measurement of Engine Power—General Requirements. 2nd ed. ISO: Geneva, Switzerland, 2016.
28. Kline, S.J.; McClintock, F.A. Describing Uncertainties in Single-Sample Experiments. *Mech. Eng.* **1953**, *75*, 3–8.
29. de Melo, T.C.C.; Machado, G.B.; Belchior, C.R.; Colaço, M.J.; Barros, J.E.; de Oliveira, E.J.; de Oliveira, D.G. Hydrous ethanol–gasoline blends–Combustion and emission investigations on a Flex-Fuel engine. *Fuel* **2012**, *97*, 796–804. [CrossRef]
30. de Oliveira, A. Análise dos Efeitos do Tempo de Injeção Direta de Etanol em um Motor Diesel Adaptado Para Operação Com Bicombustível [Analysis of the Effects of Ignition Time of Ethanol Injection in a Diesel Engine Adapted for Dual Fuel Operation]. Ph.D. Thesis, Pontifical Catholic University of Minas Gerais, Belo Horizonte, Brazil, 2018.
31. He, B.-Q. Advances in emission characteristics of diesel engines using different biodiesel fuels. *Renewable and Sustainable Energy Rev.* **2016**, *37*, 570–586. [CrossRef]
32. Turns, R.S. *Introdução à Combustão: Conceitos e Aplicações*, 3rd ed.; AMGH: Porto Alegre, Brazil, 2013.

Disclaimer/Publisher's Note: The statements, opinions and data contained in all publications are solely those of the individual author(s) and contributor(s) and not of MDPI and/or the editor(s). MDPI and/or the editor(s) disclaim responsibility for any injury to people or property resulting from any ideas, methods, instructions or products referred to in the content.